Latin American Journal of Solids and Structures
www.lajss.org

Mechanical models of the behaviour of plastic materials: influence of time and temperature

Abstract

Modelling the mechanical behaviour of plastics in the simulation of phenomena involving large strains and large displacements, as in crash simulations, is a complex task due to the highly non-linear characteristics of these materials. Moreover, non negligible influences of strain-rate, multiaxial loading, and temperature are present and must be taken into account accordingly. This work presents some results about the modelling of these effects for a thermoplastic used in automotive components. The model was developed based on experimental results obtained in different loading conditions, with different temperature and strain-rate. The time factor was investigated both in short term loading (dynamic loading) and long term tests (creep loading). Both these loading cases are very important in plastic parts design.

Keywords

behaviour modelling of materials, crash, plastic materials.

M. Avalle*, M. Peroni and A. Scattina

Politecnico di Torino, Department of Mechanics, Corso Duca degli Abruzzi, 24 – 10129 Torino Italy

Received 15 Nov 2009;
In revised form 26 Jan 2010

* Author email: massimiliano.avalle@polito.it

1 INTRODUCTION

Plastic materials are gaining more and more importance also in structural and mechanical applications, where usually, metallic materials have been used. In automotive, for example, apart from many interior parts there is a growingly presence of car body parts made of different polymers, even in mass production vehicles: in addition to bumpers and hatches, there are many cases of substitution of metal sheet fenders with plastics versions. These applications will be soon followed by hoods and other large sheet parts [9]. The substitution with plastic materials is mainly due to the need for weight reduction, in particular for the body-in-white, but also for economic reasons due to the great increment of metal price (due to both the raw material cost and the energy transformation costs).

The substitution of metals with thermoplastics in the automotive field is not a straightforward process but it brings significant complications for the designers. In addition to the different manufacturing and assembly technology, the plastic materials have very different mechanical behaviour and physical properties, both much more complex under different points of view.

One of the more complicated problems, for the numerical analyses used in structural verifications, is related to the strongly non-linear behaviour which must be taken into account when studying impact problems such as, for example, those occurring during accident. These problems are ever more important, aiming to improve first the safety of vehicle passengers, and also the safety of other road users like pedestrians and cyclists (vulnerable road users). The pedestrian protection is an up-to-date topic in car design, mainly, but not only, due to the introduction in Europe of stricter regulations and, in particular, European Directive 2003/102/CE. Because of these new rules, the front parts of all vehicles should be less aggressive against pedestrians, both adult and child. The parts involved in the redesign for this regulation are the bumpers, the bonnet, and the windscreen as well as all the connected parts and, in a certain way, also the top of the engine [6].

For what concerns the construction of bumpers, as well as other car parts, the *Thermoplastic Olefinic Elastomers* (TPO, or *Poly-Olefinic Elastomer*, POE) are very interesting materials. They are extremely versatile plastic materials, with very low cost, excellent moldability, and good resistance to several environmental agents. Its structure combines the advantages of crystalline polyolefins, with good mechanical strength, and remarkable ductility due to the olefinic rubber phase. These two fundamental properties can be widely changed by using different percentage of the two basic components.

TPO's mechanical behaviour, as for the other thermoplastic materials, is quite complex, for this reason the numerical simulations of phenomenon such as crash, need numerous steps. First of all, an experimental characterization of the mechanical behaviour in different test conditions is needed: the first effect to keep into consideration is the time influence, and in particular strain-rate effects. Moreover, the temperature effects and the multi axial loading influence must be taken into account. Then, it is necessary to determine the mechanical material parameters of the adopted model. In fact, adequate simulation models of the mechanical behaviour, implemented in the numerical codes, have to be used.

In this work the characterization of a TPO for automotive applications has been carried out. A detailed experimental tests campaign covering the main influencing factors has been first fulfilled. The experimental results were used to obtain the parameters for a suitable model implemented in a numerical code. Some of the most interesting analytical and empirical models available in the literature are also examined and discussed. The explicit LS-DYNA solver for the dynamic simulations and the implicit LS-DYNA and Abaqus solvers for creep simulations have been used. Long term analysis is also necessary for car body parts since it is quite usual to have very high temperatures, up to 70-80°C or even more, in normal use: softening and creep cannot be neglected in these environmental conditions.

Good fitting of the numerical to the simulation results has been obtained and the results provide a very useful tool for the design of automotive plastic body parts.

2 MECHANICAL BEHAVIOUR OF PLASTIC MATERIALS

A detailed and comprehensive model for the mechanical behaviour of a plastic material has to take into account several basic aspects and needs the definition of a series of elements such as a yield surface [8, 10, 17, 21, 27, 28, 33], a hardening law, anisotropy, visco-elastic and visco-plastic behaviour, and environmental effects.

Even if the third topic is not negligible in general, it will not be addressed in this work. Anisotropy is, in this case, a second level of approximation far less important than the other. The yield surface is also not addressed since the usual Von Mises approximation is adequate for most simulations [5, 14, 18].

The material hardening and the viscous behaviour, not negligible in plastics as is usually assumed for metals, can be modelled in an effective way by means of elastic/viscous element chains put in series/parallel according to different combinations [2–4, 7, 24, 26, 32, 34, 35]. These models are mainly for hyperelastic materials, however, without plastic deformation included.

Modelling the elasto-plastic behaviour is crucial for any formulation. Many theoretical and semi-empirical relationships have been proposed. The experimental stress-strain curve is often used as well.

In 1979 G'Sell and Jonas [13] obtain, for PVC and HDPE, an explicit form for the true stress as a function of the effective plastic strain:

$$\sigma\left(\varepsilon,\dot{\varepsilon},T\right) = Ke^{\left(\gamma_e/2\varepsilon_p^2\right)}\dot{\varepsilon}^m f\left(T\right) \tag{1}$$

The influence of strain-rate is also modelled with a simple but effective power law. This formulation, however, has the drawback of predicting a stress-strain curve lower than that obtained at a reference speed at decreasing strain-rates. The influence of temperature is modelled by a multiplication term $f(T)$ that will be discussed later.

The passage from the elastic regime to yielding is abrupt, unlike in real tests. A more realistic model is given in [12]:

$$\sigma\left(\varepsilon,\dot{\varepsilon},T\right) = Ke^{\beta/T}\left(1-e^{-w\varepsilon_p}\right)e^{h\varepsilon_p^q}\dot{\varepsilon}^m f\left(T\right) \tag{2}$$

In (2) temperature effect is taken into account by the first multiplying factor. The second term describes the low plastic strain behaviour, whereas the third term account for the high plastic straining. Finally the fourth term takes into account the strain-rate of the material using a Norton-Hoff law.

Lauro and Oudin [22] propose instead the quadratic approximation:

$$\sigma\left(\varepsilon,\dot{\varepsilon},T\right) = Kp\left(1-e^{-w\varepsilon_p}\right)\left(1-h_1\varepsilon_p+h_2\varepsilon_p^2\right)\dot{\varepsilon}^m f\left(T\right) \tag{3}$$

In 2007 Peroni and Avalle [30] propose a more flexible model based on a double power function law:

$$\sigma(\varepsilon,\dot{\varepsilon},T) = \left(A + k_1\varepsilon_p^{n_1} + k_2\varepsilon_p^{n_2}\right)\left[1 + \left(\frac{\dot{\varepsilon}}{D}\right)^{1/m}\right] f(T) \tag{4}$$

For what concerns the strain-rate effect, the Cowper-Symonds model (the term within square brackets in Eq. (4)) was found acceptable for many semi-crystalline and amorphous polymers [1, 25].

From version 9.50 of the LS-DYNA code [11] a material model *MAT_106, able to couple the mechanical and thermal behaviours has been implemented. The formulation of the stress-strain relationship is expressed by a series:

$$f(\varepsilon) = \sigma_0 + Q_{r1}\left(1 - e^{-C_{r1}\varepsilon_p}\right) + Q_{r2}\left(1 - e^{-C_{r2}\varepsilon_p}\right) + Q_{\chi 1}\left(1 - e^{-C_{\chi 1}\varepsilon_p}\right) + Q_{\chi 2}\left(1 - e^{-C_{\chi 2}\varepsilon_p}\right) \tag{5}$$

With this law it is possible to model very different behaviours according to the values of the nine coefficients, which can have positive and negative sign, and can be described as a function of temperature, that is $\sigma_0(T)$, $Q_{r1}(T)$, $Q_{r2}(T)$, $Q_{\chi 1}(T)$, $Q_{\chi 2}(T)$, $C_{r1}(T)$, $C_{r2}(T)$, $C_{\chi 1}(T)$, $C_{\chi 2}(T)$. The strain-rate effect is taken into account using the Cowper-Symonds formulation, as in Eq. (4).

Most models consider a multiplicative influence of strain-rate. However, a more complex interaction exists between the various parameters. Khan and Zhang [16] adapt their own KHL formulation developed for metals [15, 19, 20, 23] to fit the complex behaviour of PTFE:

$$\sigma(\varepsilon,\dot{\varepsilon},T) = \left[A + B\left(1 - \frac{\ln\dot{\varepsilon}_p}{\ln D_0^p}\right)^{n_1}\varepsilon_p^{n_0}\right]\dot{\varepsilon}_p^c\left(1 - T^{*m}\right) \tag{6}$$

For what concerns the temperature effects, the time-temperature equivalence is widely verified: decreasing the temperature has the same effects of an increase in the strain-rate. Both effects, for example, involve increase of yield strength and embrittlement. Such equivalence is usually considered by the Zener-Hollomon's law described by means of the homonymous parameter. Therefore the function $f(T)$ accounting for temperature effect is described by:

$$f(T) = \exp\left(\frac{Q}{RT}\right) \tag{7}$$

Equally related to the time of application of a stress field is the problem of creep. Creep occurs on a larger time scale. However, there are relations with normal load applications at slow speed: in theory quasi-static load application corresponds to a period that tends to infinity. The physical basis of creep is the same that governs strain-rate effects [31]. However, the usual engineering approach is quite different and considers a constant load application over a long time. Strain is instead the dependent variable, time being the independent variable. Therefore, stress as well as temperature, are controlling parameters.

The most effective way to implement the creep behaviour is the so called Norton law or time-hardening formulation. This law only describes the primary creep:

$$\varepsilon_{creep} = A_0 \sigma^m t^n \tag{8}$$

When $n = 1$ the secondary creep is modelled. Usually the Arrhenius formulation is used to include temperature effects, with a multiplicative approach as described above for strain-rate effects.

However, a formulation with a series of power laws allows describing the three creep phases:

$$\varepsilon_{creep} = A_0 \sigma^{m_0} t^{n_0} + A_1 \sigma t + A_2 \sigma^{m_2} t^{n_2} \tag{9}$$

The parameters in (9) are bounded by: $n_0 < 1$ and $n_2 > 1$. The second term describes the linear creep, if any.

The primary and secondary creep phases should be modelled more correctly by an exponential formulation if a linear visco-plastic model is applicable. This is not the case, as experimentally observed, in many materials and a power law approximation fits better the experimental data.

Moreover, in most of the finite element codes, and in particular in those used in this work, LS-DYNA and Abaqus, only the primary creep is implemented, mostly because it is the more important to be considered in practical applications.

3 MATERIAL UNDER STUDY

In the research presented in this work the polymer DEXFLEX 162HF by Solvay (actually produced by LyondellBasell) has been considered. DEXFLEX 162HF is an olefinic thermoplastic obtained by compounding an olefinic rubber into a matrix of polyolefin plastic (mainly PP; Figure 1). It is increasingly used for the construction of external automotive parts that need a combination of adequate stiffness, impact strength at low temperature, and good workability. Furthermore, it can be modified to be adapted to manufacturing demands. For these reasons it is widely used for bumpers especially. In Table 1 the main properties of the material are reported.

Table 1 DEXFLEX 162HF data (source: database Campus® WebView).

Property	Value	Standard Test
Elastic modulus	800 MPa	ISO 527-1/-2
Thermal expansion coefficient	$0.8 \times 10^{-4}\ °C^{-1}$	ISO 11359-1/-2
Density	950 kg/m^3	ISO 1183

The material characterization tests have been performed by using an injection moulded specimen in accordance to the standard ISO 527, type 1A, generally used to characterize plastics (Figure 2).

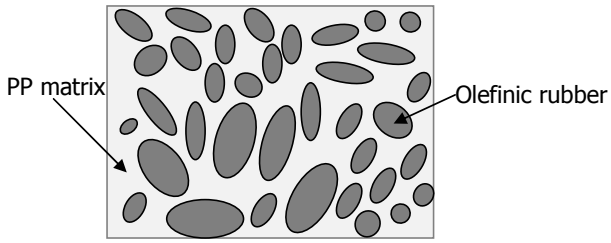

Figure 1 Schematic of the TPO structure.

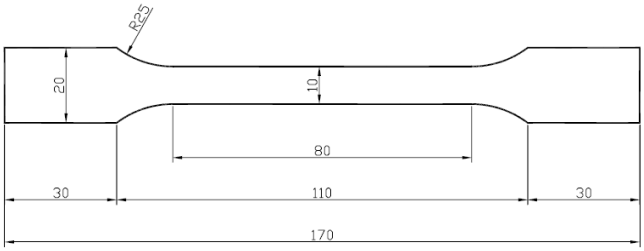

Figure 2 Specimen for plastic material according to ISO 527, type 1A. Thickness is 4 mm.

4 EXPERIMENTAL METHOD

The experimental activity has been limited to uniaxial characterization tensile tests. While, as discussed in the introduction, the triaxiality effects are in general not negligible for plastics, strain-rate and temperature effects – fundamental for the current application – are very difficult to study in complex loading combinations. In the application under study, related to impact deformation of car body parts, strain-rate can go, locally, up to several hundredths of s^{-1}, with temperatures ranging from -40°C to +100°C. Finally, most models implemented in the codes (like LS-DYNA) are unable to take into account the influence of a hydrostatic state of stress.

The quasi-static and dynamic tensile tests have been performed by means of three experimental testing devices [27, 28, 30]. These experimental devices are:

1. Zwick Z100: electro-mechanical universal material testing machine with a maximum load of 100 kN, used for low strain-rate tests

2. DARTEC HA100: universal servo-hydraulic material testing machine, with the same 100 kN maximum load, for medium strain-rate tests (a lower range load-cell, 10 kN maximum, was used in the tests)

3. FasTens: a pneumatically actuated mechanical testing machine, for tests loading up to 15 m/s. It is a custom device built within the Safety and Reliability Laboratory of the Second Faculty of Engineering of Politecnico di Torino, in Vercelli site [27–29] (Figure 3)

The principle of operation of FasTens is as follows: a pneumatic actuator is loaded with pressurized air (maximum pressure is 10 bar). Energy is accumulated in the chamber until

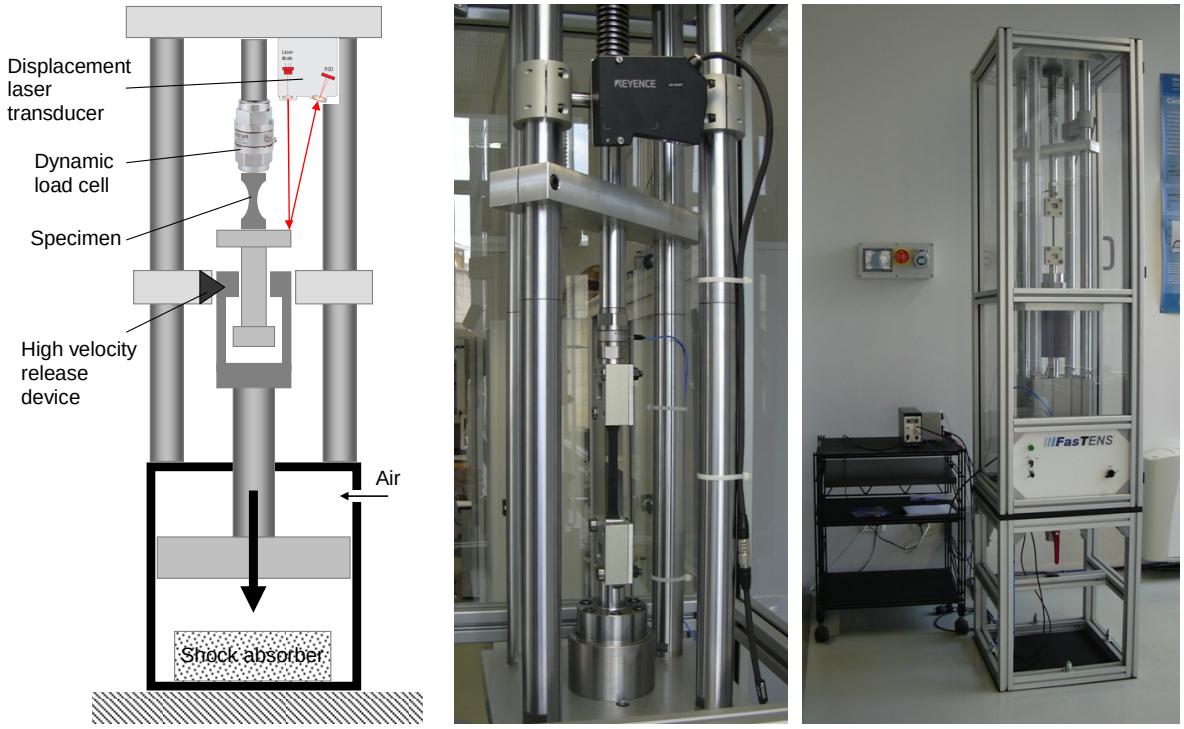

Figure 3 FasTens pneumatically actuated tensile testing machine.

breaking of a linkage bar occurs. The piston is then accelerated and catches the moving fixture attached to the sample. The load is measured by a piezoelectric load cell (Kistler 9341, 30 kN range), whereas the displacement is measured by a triangulation laser transducer (Keyence LK-G407, with 100 mm measuring range and a 50 kHz bandwidth).

The tests at various temperatures were done by means of a climatic cell, specifically constructed for the testing machines described above (Figure 4). This climatic cell has a sandwich structure with two external aluminium sheet and a core of polyurethanic foam. Temperature in the cell is monitored by a thermocouple (type K) and a National Instruments acquisition board in a PC. To perform the temperature conditioning in the adopted range (-40 to +80°C) a pneumatic system called Vortex tube® has been used. To accurately control the temperature of the cell, a close-loop control has been developed that act on an electronic-pressure regulator feeding the Vortex tube®. In this way it is possible to precisely control the temperature in climatic cell also during slowest mechanical test that lasts more than ten minutes.

The creep tests were done with the Zwick Z100 machine (for the faster tests) and with a custom pneumatic testing equipment shown in Figure 5 (for longer time tests). This equipment is based on a pneumatic actuator controlled in closed-loop by a load feedback system. This type of equipment, apparently more complicated than a classical weight loading system, is much more flexible and compact.

The tensile tests were only partially in conformity to the ISO 527 standard. In fact, this

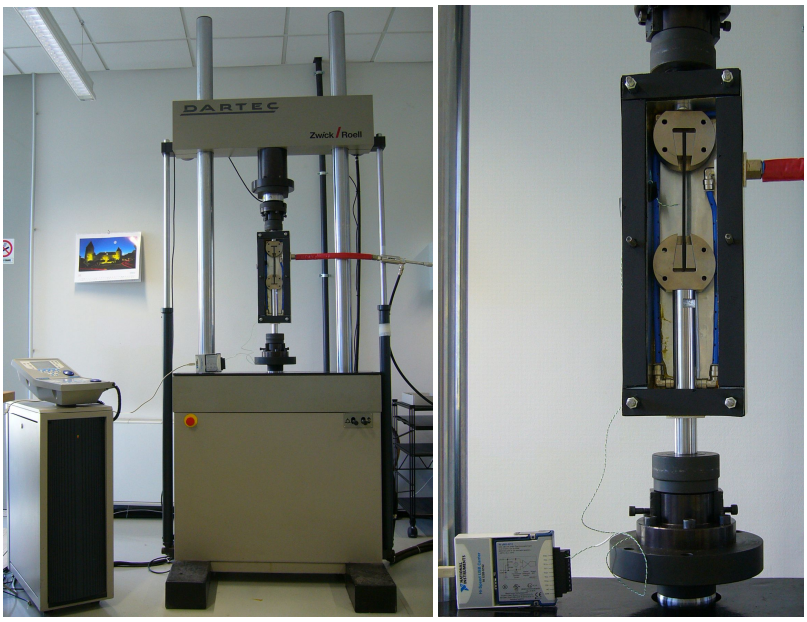

Figure 4 Test chamber for low, down to -40°C, and high, up to +100°C, temperature tests on plastic materials

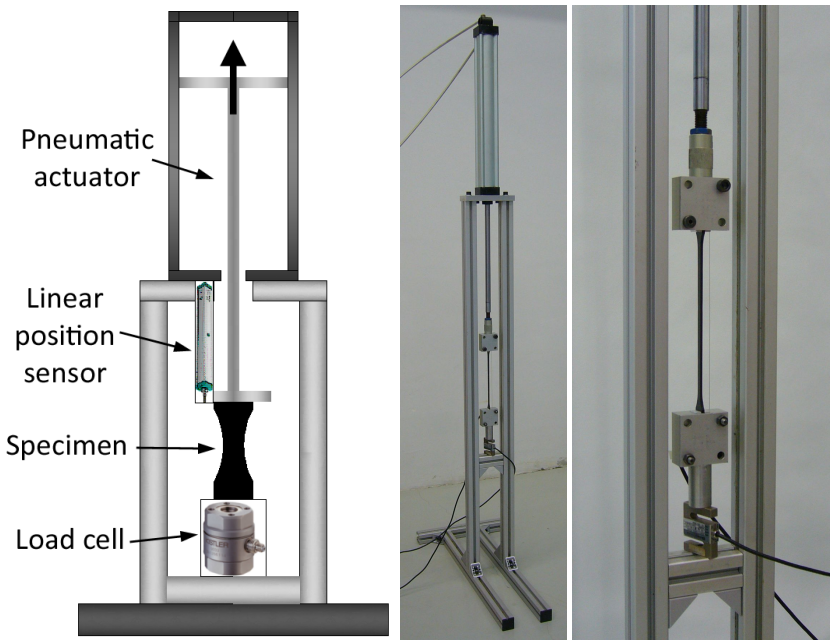

Figure 5 Creep testing equipment.

standard does not consider high strain-rate testing. The strain-rate, instead, is preferably constant in the current tests, at largely dissimilar values. In addition, the loading mode of the three devices required to cover the interesting range of strain-rate, is different: this is not avoidable by any means.

5 EXPERIMENTAL RESULTS

5.1 Tests at different strain-rate and temperature

In Figure 6 the results of the tests as a function of temperature, for two values of strain-rate, are shown. In Figure 7 some specimens after tensile tests at different loading speed are shown: at room temperature ductility falls off at loading speeds greater than 10 mm/s, corresponding to a strain-rate about 0.1 s^{-1}.

Figure 8(a), instead, is aimed to illustrate the influence of the strain-rate at constant (room) temperature.

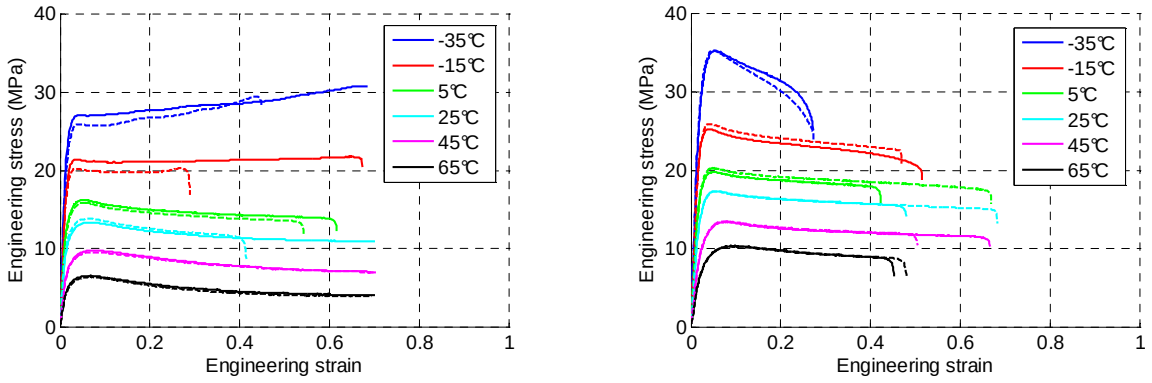

(a) (b)

Figure 6 Effect of temperature on the tensile characteristics of DEXFLEX 162HF at (a) very low strain-rate, 5×10^{-3} s^{-1} and (b) low-medium strain-rate, 0.5 s^{-1} (continuous and dashed lines are replications of the same test).

It is clear that the previously discussed analogy between strain-rate and temperature effects is confirmed: decreasing the temperature has the same effects that increasing strain-rate. In details, increasing the strain-rate decreases the toughness and increases the yield stress, and vice-versa.

The Young modulus, Figure 8(b), is equally affected: a linear decrease of Young modulus with increasing temperature is observed, for both strain-rate values, 0.5 mm/s and 50 mm/s. On the other hand, no substantial influence of strain-rate on Young modulus is observed: in addition, measure uncertainty on Young modulus in high strain-rate testing does not normally allow to correctly evaluate it.

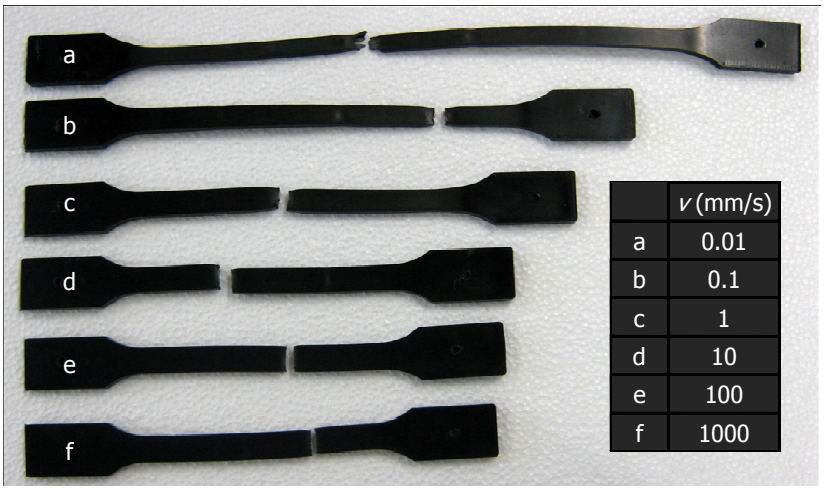

Figure 7 Samples of the DEXFLEX 162HF material after tests.

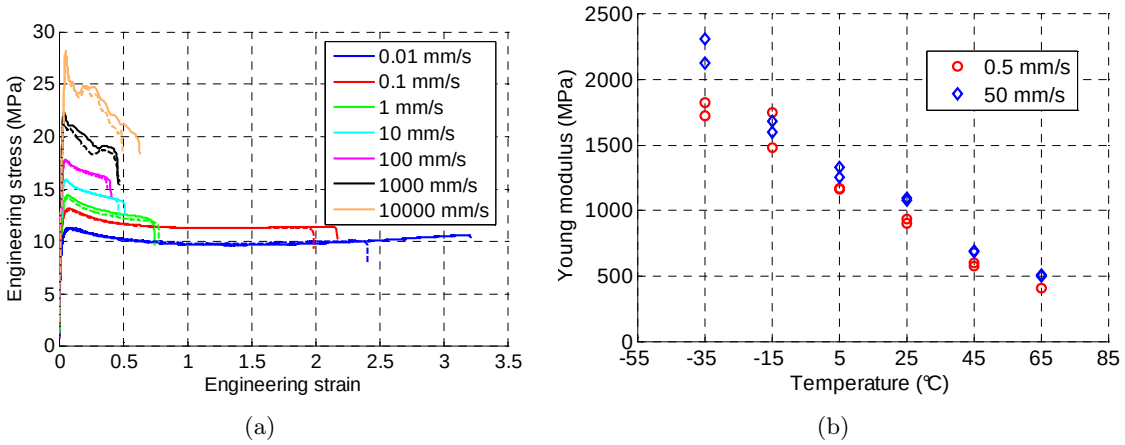

(a) (b)

Figure 8 (a) Effect of strain-rate on the ambient temperature characteristic of DEXFLEX 162HF (continuous and dashed lines are replications of the same test) and (b) Effect of temperature on the elastic modulus of DEXFLEX 162HF at two values of strain-rate.

The combined effect of temperature and strain-rate on the maximum stress is illustrated in Figure 9. The experimental results are well fitted by the Cowper-Symonds formulation, with $D = 15.2\ s^{-1}$ and $p = 5.32$, for the strain-rate effect and, for the temperature, by the Johnson-Cook model ($m = 0.51$) as in Eq. (6).

To prove the effectiveness of model (5), Figure 10(a) reports the analytical fit of the true stress-true plastic strain curves obtained from tensile tests performed at 0.5 mm/s and previously shown in Figure 7(a). Figure 10(b) shows the three parameters of the model as function of test temperature. It is necessary to underline that this kind of analysis is effective only at low strain-rate because at higher strain-rate values, thermal-softening phenomena prevent correctly extracting the model parameters.

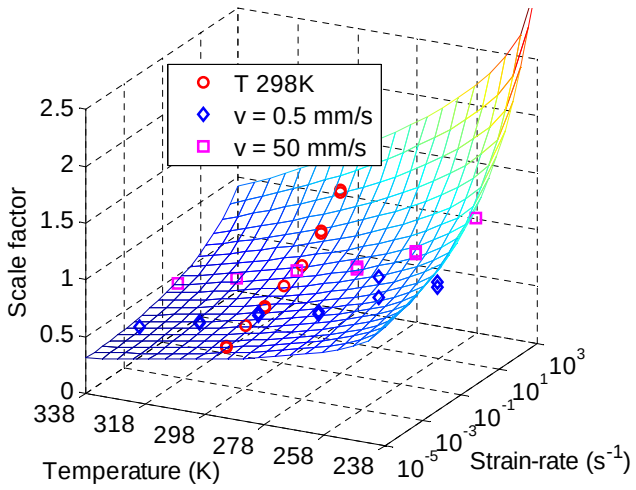

Figure 9 Interpolation surface for the maximum load of DEXFLEX 162HF as a function of temperature and strain-rate

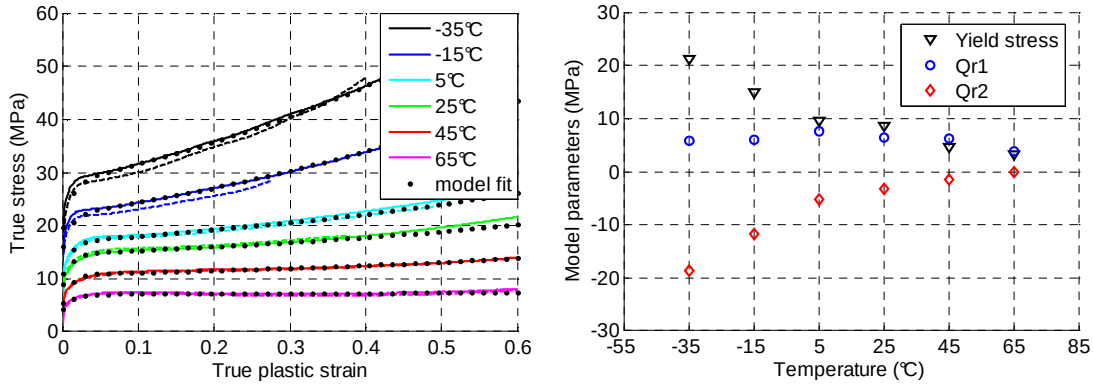

(a) (b)

Figure 10 (a) Model parameter as function of test temperature and (b) comparison between experimental true stress-true plastic strain curves and analytical fit.

Besides, the evaluation of the Poisson ratio of the examined material was obtained using an optical measuring technique based on the speckle method and on DIC (*Digital Image Correlation*). Figure 11 illustrates the variation of the Poisson ratio as a function of test time, compared to stress. It can be noted that the Poisson ratio, initially close to 0.5 in the elastic range, decreases progressively at yield, then continues decreasing to reach an asymptote for very high strain.

The constant volume hypothesis is no more valid for these materials in the plastic regime: the growth of micro voids becomes very important at the higher stages of deformation and the usual plasticity formulation of metals loose validity. As it will be discussed in the section regarding the numerical simulations, this aspect is completely neglected by most material

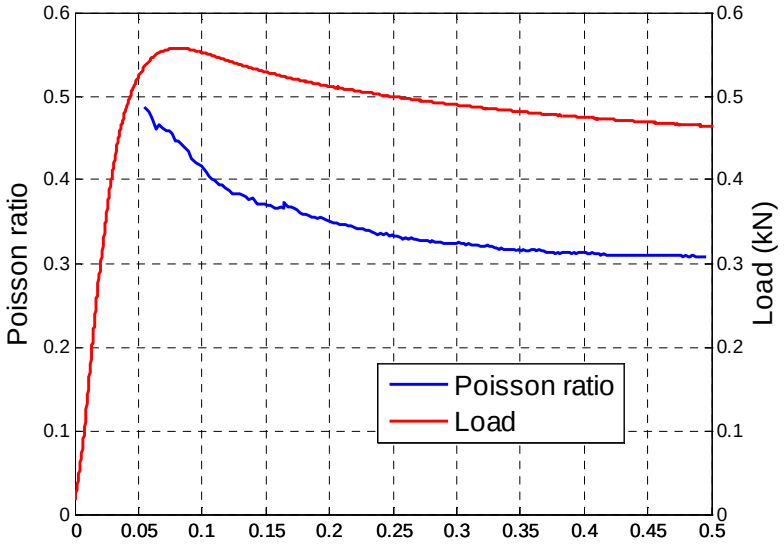

Figure 11 Variation of Poisson ratio during a tensile test.

models implemented in commercial FE codes, and this can affect the calculations. Fortunately, this is a secondary effect negligible in most simulations.

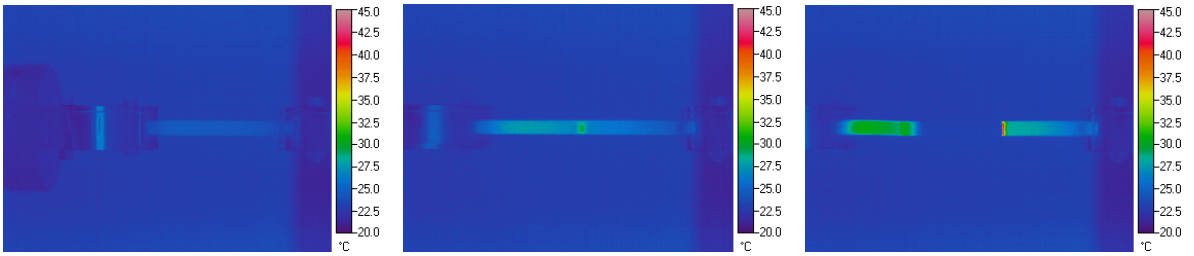

Figure 12 Thermo-photos sequence of a tensile tests performed at 100 mm/s.

Finally, Figure 12 shows the important phenomenon of thermal softening that can occur in high strain-rate tests and that cannot be neglected in numerical simulations. In particular, Figure 12 proposes a sequence of thermal images taken during a tensile test performed at 100 mm/s at room temperature. As it is easy to note, the specimen temperature can increase of about 25 °C at this velocity where the strain is localised. As shown in Figure 7, this causes a not negligible reduction of material strength that must be suitably kept into account with a coupled thermo-mechanical numerical simulation.

5.2 Creep tests

In Figure 13 the results of a series of creep tests are reported, at levels of the applied constant load ranging from 6.25 MPa to 9.375 MPa, in eight equal steps. As it is possible to note, this material, more notably at higher loads, does not show a secondary creep phase – see also the

detailed view in Figure 13(b). This consideration is confirmed when fitting the experimental data with the creep law described by (9): by using least square approximation, it has been observed that the parameter A_1, corresponding to the linear creep, is always negligible (Figure 14). It is interesting to observe how the parameters of equation (9) that governs primary and tertiary creep, change as a function of the applied stress (Figure 14) and are well fitted by the equation (9) itself.

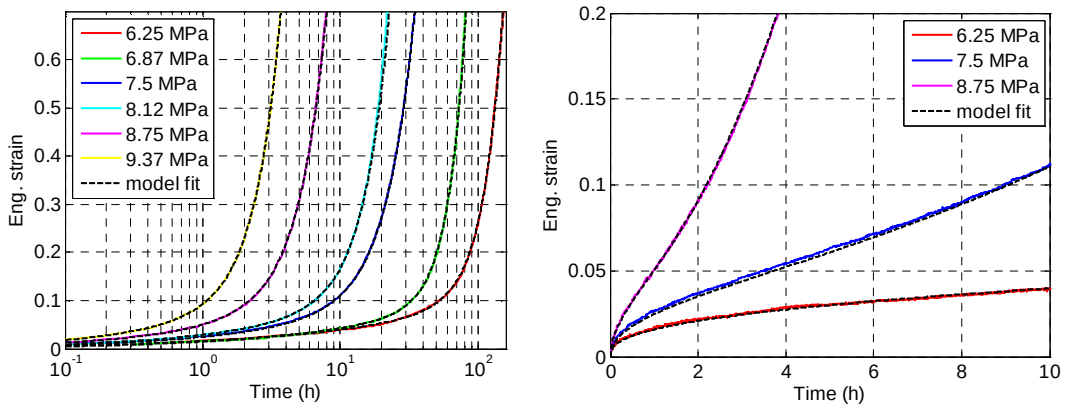

(a) (b)

Figure 13 (a) Effect of stress on the room temperature creep characteristic (strain as a function of time) of DEXFLEX 162HF; (b) detailed view of the first part for some of the curves.

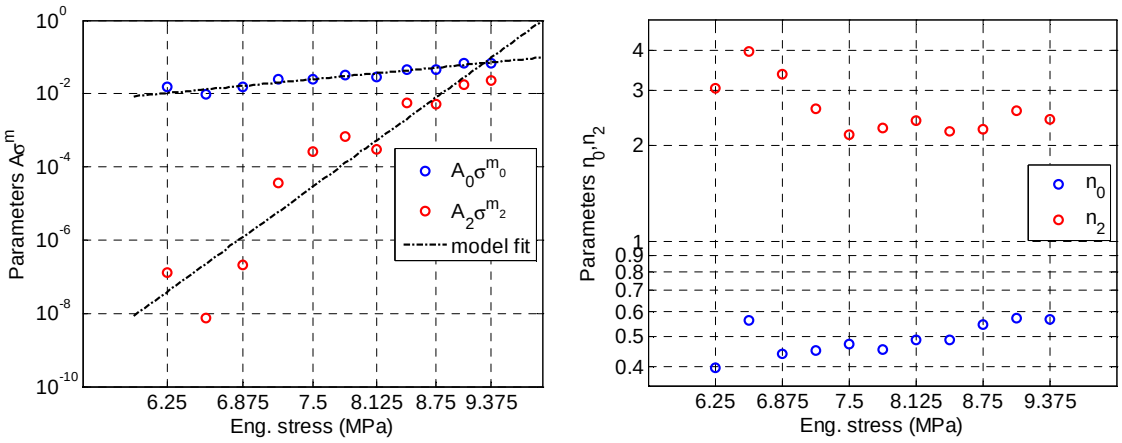

(a) (b)

Figure 14 (a) Trends of $A_0\sigma^{m_0}$ and $A_2\sigma^{m_2}$ products and (b) n_0 and n_2 as a function of the applied stress.

6 NUMERICAL MODELLING

6.1 Influence of strain-rate and temperature

All the simulations aimed to study the influence of strain-rate and temperature on the mechanical behaviour of DEXFLEX 162HF have been done with the explicit/implicit FEM code LS-DYNA, version 9.71, modelling a quarter of the specimen. Full integrated eight-node hexahedrical elements and the implicit solver have been used for low-speed tests. Besides, the explicit solver has been used for high-speed tests simulations. To take into account both the temperature and the strain-rate effects, a specific material model for plastics has been adopted. This model is implemented in the LS-DYNA code and, specifically, it is the so-called *MAT_ELASTIC_VISCOPLASTIC_THERMAL (*MAT_106) suitable for coupled thermo-mechanical simulations. A main drawback of this model for plastics lies in the fact that it is not possible to take into account the influence of the hydrostatic component of stress on yield: despite this, a careful evaluation of several alternative models suggested *MAT_106 as an optimal compromise between the modelling accuracy and the complexity in identifying the model parameters. Moreover, experimental evidence (Figure 15) demonstrated that, for this specific material the ratio between the strength in tension and in compression is relatively not too far from one so that the simple Von Mises yield criterion seemed an acceptable approximation.

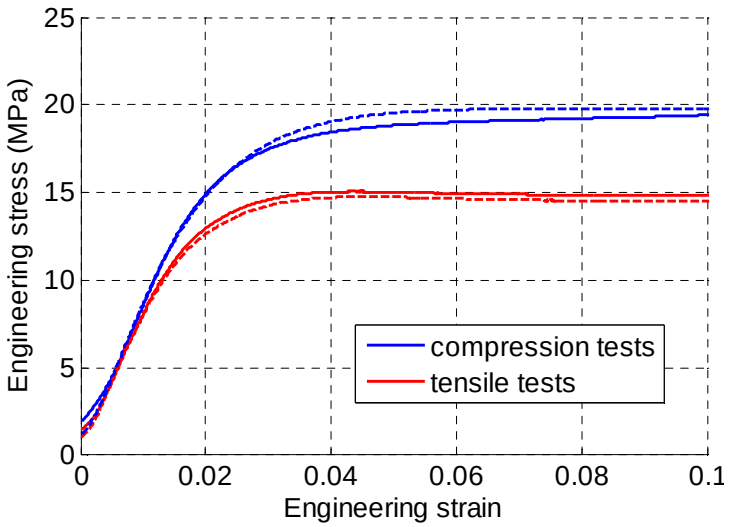

Figure 15 Comparison of the tensile with the compressive behaviour of the material (the curves with dashed lines are replications of the same test).

The coefficients of this model at different strain-rates and temperatures have been derived from the experimental tests with an inverse numerical procedure [29, 30]. The procedure aims to find the correct value for the material properties by minimizing the error between the calculated response and the experimental result. The error is evaluated by comparing the global engineering stress-engineering strain curves (or alternatively the load-stroke characteristics

obtained from the specimen): doing so, it was not necessary to have a detailed experimental evaluation of the local strain field as explained in the previous section 4.

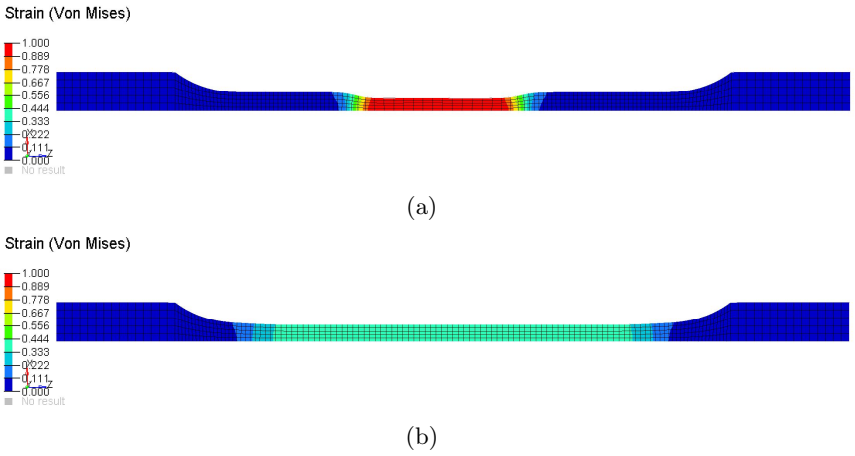

Figure 16 Example of the results obtained when (a) excluding or (b) activating the viscous effect modelling.

The error is evaluated by some significant estimator: usually, as it was chosen in the current work, the total squared error sum is used. As a matter of fact, the method applies an iterative solution algorithm to the non-linear least square problem of approximation of the experimental response. For this purpose the optimization software Altair HyperStudy® has been used.

.

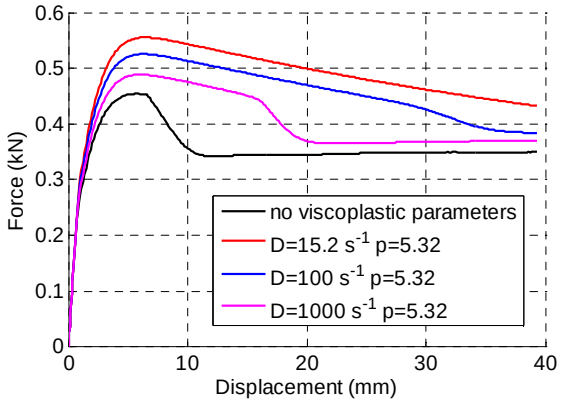

Figure 17 Example of the comparison between the results obtained from the numerical model when activating or excluding viscous effects.

Before analysing in details the results obtained with the proposed numerical procedure, it is necessary to underline an important observation from Figures 16 and 17. When viscous effects are neglected, by zeroing the strain-rate effects parameters, mechanical behaviours simulated with numerical models became more similar to that of an amorphous polymer, such as for

example polycarbonate: in particular, the material shows local necking that propagates along the restricted section length until the total central region is fully yielded, as in Figure 16(a). Usually these materials are less influenced by strain-rate than crystalline [30]. In this case, the load-displacement characteristic shows a marked decrease after yield and a large plateau corresponding to progressive yielding and neck propagation, with continuous elongation of the restricted region of the specimen, as in Figure 16 that shows the comparison of some numerical force-displacement curves obtained with different viscosity parameter (Cowper-Symonds formulation).

On the other hand, with greater strain-rate sensitivity the smoother curves are obtained: the red curve is obtained using Cowper-Symonds parameters extracted analytically from experimental data. When strain-sensitivity is included, the simulated behaviour becomes actually similar to DEXFLEX 162 HF, a highly crystalline polymer with great strain-rate sensitivity. In this case the phenomenon of localized necking and its propagation is less evident and the load-displacement curve shows a typical monotone smooth decrease. This phenomenon is obtained even introducing a monotonically increasing true stress-effective plastic strain characteristic, that is, even without softening (that has the side effect of numerical instability). In this type of test, the strain-rate decreases during the test and it cannot be kept constant along the specimen. Instead, the high strain-rate sensitivity of the material tends to lock the onset of necking because local necking would induce a sudden acceleration of strain: the material then responds with a stress increase, or at least stabilization, blocking further local necking.

For what concern strain-rate sensitivity *MAT_106 model is not particularly effective because it keeps into account the strain-rate influence on yield stress only and only allows for the Cowper-Symonds visco-plastic formulation For these reasons, the experimental force-displacements curves are not reproducible with this model, Figure 18(a), because the parameters C_{r1} and C_{r2} are constant at different strain-rate values. On the other hand, the numerical model fit very well the maximum load (except for the low strain-rate tests) as shown in Figure 18(b).

For what concerns thermal sensitivity *MAT_106 model allow to efficiently describe the material behaviour. In fact all material model parameters can be defined as functions of temperature. In Figure 19(a) the comparison of experimental force-displacements curves obtained at different temperature at 0.5 mm/s is presented with the fit obtained from the optimization procedure. In Figure 19(b) are the material parameters of *MAT_106 model as a function of temperature are shown.

It is worth to note that the parameters obtained in Figure 10(b) and 19(b), obtained from the same experimental tests, are not equivalent because the last were obtained from the FE model and the optimization procedure, thus keeping into account the actual field of stress, strain, strain-rate, and temperature. The final results in terms of the model coefficients are summarised in Table 2.

Besides, three main limitations of the material model used should be mentioned. The first relates to the fact that this material routine includes the storage volume in plastic field: this is in contradiction with the evidence of experimental results (Figure 11). Moreover, this model

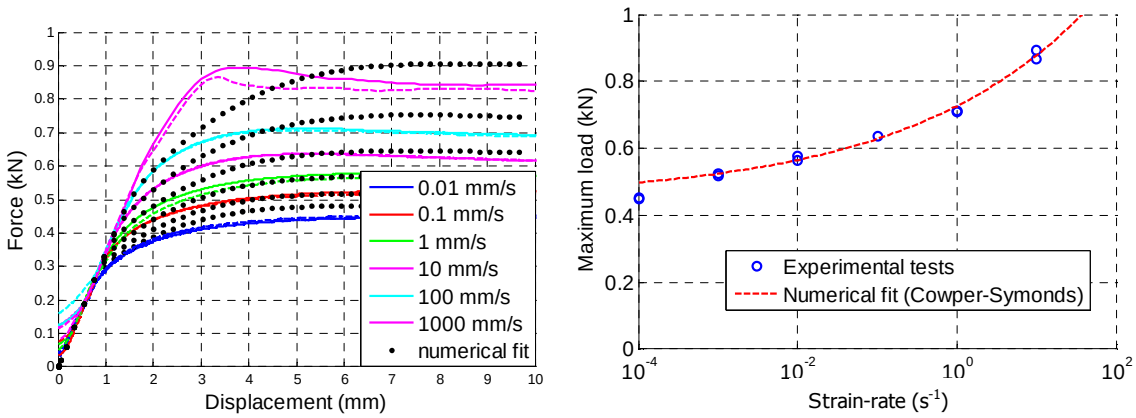

(a) (b)

Figure 18 Evaluation of strain-rate sensitivity with the numerical procedure: (a) comparison of force-displacement curves and (b) evaluation of the Cowper-Symonds fit of the maximum load.

provides a Von Mises yield surface that does not fit properly the plastic material behaviour that can be sensitive to the hydrostatic stress. In this regard, models such as the SAMP-1 (Semi Analytical Model for Polymers) [21] could properly address this two issues. However, SAMP-1 is a very complex model needing much more experimental tests and quite difficult to identify in all the necessary parameters. A preliminary investigation using this model was done and abandoned due to these difficulties. Moreover, the preliminary results obtained did not show much improvement. The last inconvenient of *MAT_106 model is computational instability, especially in coupled thermo-mechanical analyses: many other numerical problems have been encountered during the results fitting, such as lack of convergence for higher strain values, especially with the implicit solver.

It is important to underline that the proposed optimization procedure allows to precisely keep into account thermal-softening phenomena occurring in high strain-rate tests. This result is easy to achieve with a preliminary calibration of the numerical model (it is necessary to evaluate the amount of plastic work converted into heat) and by using a FEM solver that allow performing coupled thermo-mechanical simulations.

Table 2 Identified parameters of the *MAT_106 material law.

Temperature(°C)	Yield stress(MPa)	Q_{r1}(MPa)	Q_{r2}(MPa)	C_{r1}	C_{r2}
-35	14.0	7.83	-11.48	110	-1.38
-15	12.2	5.73	-8.69		
5	8.8	4.84	-4.37		
25	6.8	4.61	-3.48		
45	4.2	3.87	-2.46		
65	2.3	3.28	-1.16		

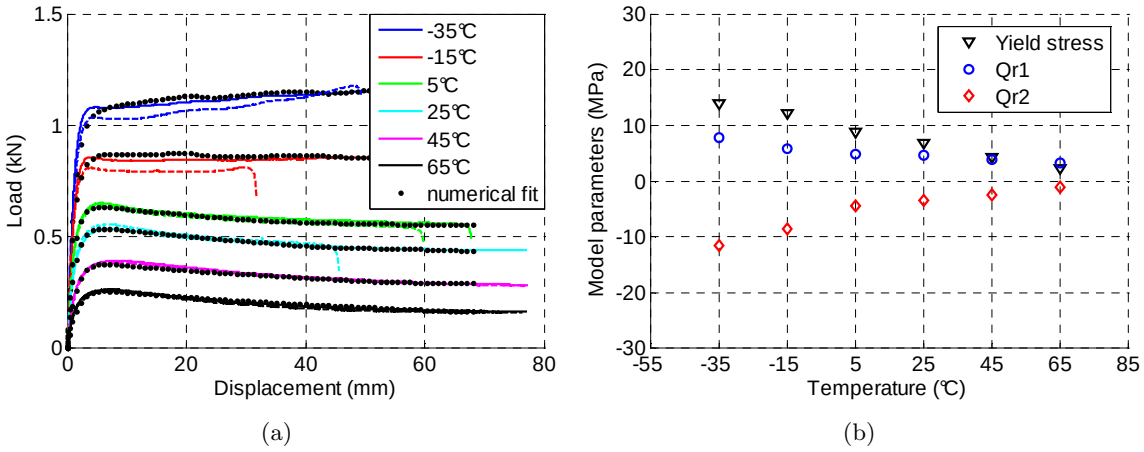

(a) (b)

Figure 19 Evaluation of thermal sensitivity with numerical procedure: (a) comparison of force-displacement curves and (b) material parameters of *MAT_106 model depending on temperature.

6.2 Creep behaviour simulation

For creep simulation, two different commercial codes, the already mentioned LS-DYNA and Abaqus, were used with the implicit solver. To simulate the experimental creep tests a material model that implements the Norton law (8) was chosen for both codes, in particular, for LS-DYNA it was the *MAT_UNIFIED_CREEP. With this formulation it is possible to model only the primary creep: moreover, the codes allow modelling the temperature influence.

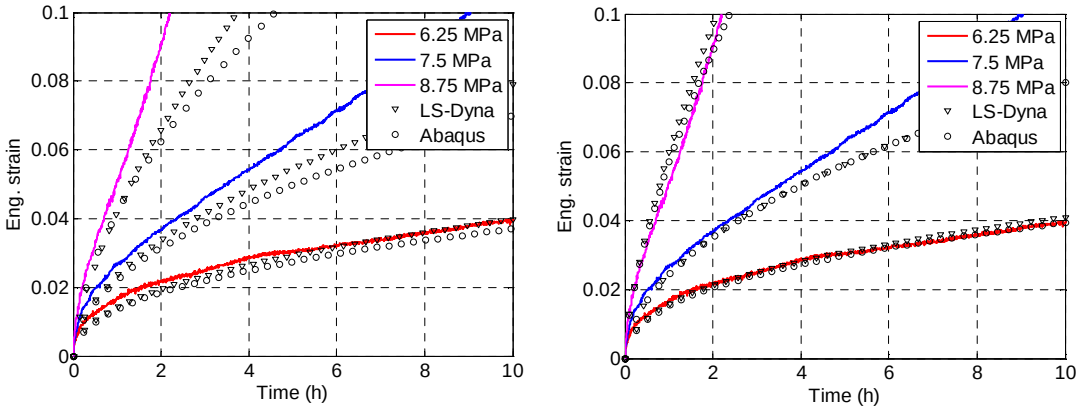

(a) (b)

Figure 20 Comparison between experimental and numeric curves at different stress level, obtained with a global fit (a), and fitting the primary creep only (b).

The material parameters A_0 and m which have to be introduced in the material models have been obtained by fitting the experimental curves as shown in the previous section. The simulations were performed on the same specimen shown in Figure 2. In this case also, the FEM model was restricted to a quarter to save computational time and applying the appropri-

ate constraints. All the experimental creep tests in the illustrated stress range were simulated, obtaining a good agreement between the numeric curves and the experimental ones. In particular, as shown in Figure 20(a) the numeric curves progressively underestimate the strain because tertiary creep phase is not modelled. To obtain better results, at least at lower strain, the fit with the Norton law should be restricted to primary creep on the experimental curves directly.

7 CONCLUSIONS

The mechanical behaviour of a thermoplastic material used in automotive body parts has been examined in this work. The combined effects of the temperature and time factor on the stress-strain characteristic have been studied. This material, as for all thermoplastics, is strongly affected by both external influencing factors.

The experimental analysis has been done with tests at different strain-rates, creep tests, and tests at different temperatures in the range of operation for the applications of interest, usually -40°C to +100°C. For the applications that are aimed for this materials, the dynamic behaviour is particularly important: for this reason, the numerical modelling has been done with an explicit solver while, for the creep part, an implicit formulation has been chosen. The available models allow to represent in a proper way the mechanical behaviour of material as a function of strain-rate and temperature, in a visco-plastic flow regime. Identification of the material properties and a general representation of the material behaviour were found with acceptable predictability over the entire range of external conditions. The time and temperature effects, for short time tests can be modelled with a good precision. The load effects on longer time scale tests can be described with less precision because, as far as the current models are available, they are able to consider the primary creep only.

Still a generic formulation that allows modelling in a synthetic way the material in all the operative conditions is not available. However, this is only a partial lack for many applications in simulations for automotive, both of dynamic phenomena and long term load applications.

References

[1] M. Alves. Material constitutive law for large strains and strain rates. *J. of Eng. Mech.*, 8:126–215, 2000.

[2] N.M. Ames, V. Srivastava, S.A. Chester, and L. Anand. A thermo-mechanically coupled theory for large deformations of amorphous polymers. Part II: Applications. *Int. J. of Plasticity*, 25:1495–1539, 2009.

[3] E.M. Arruda and M.C. Boyce. Evolution of plastic anisotropy in amorphous polymers during finite straining. *Int. J. of Plasticity*, 9:697–720, 1993.

[4] E.M. Arruda, M.C. Boyce, and R. Jayachandran. Effects of strain rate, temperature and thermomechanical coupling of the finite strain deformation of glassy polymers. *Mech. of Mat.*, 19:193–212, 1995.

[5] B. Bader and R. Koch. Numerical simulation (FEM) of snap-in and snap-out processes of ball snap-fits. *Comp. Mat. Sci.*, 3:125–134, 1994.

[6] B.M. Boggess, J. Wong, and S. Mark. Development of plastic components for pedestrian head injury risk reduction. In *Proc. XVIII ESV Conference*, 2002. Paper No. 294.

[7] M.C. Boyce and E.M. Arruda. An experimental and analytical investigation of the large strain compressive and tensile response of glassy polymers. *Polymer Eng. and Sci.*, 30(20):1288–1298, 1990.

[8] B. Farrokh and A.S. Khan. The yield locus of a thermoplastic polymer. In *Proc. Plasticity 2007 (International Symposiums on Plasticity and its Current Applications)*, Alaska, 2007. Anchorage.

[9] F.I.M. Geoff Davies. *Materials for Automobile Bodies*. Elsevier, Oxford, 2003.

[10] E. Ghorbel. A viscoplastic constitutive model for polymeric materials. *Int. J. of Plasticity*, 24:2032–2058, 2008.

[11] B. Gladman et al. *LS-DYNA® Keywords user's manual – Volume 1*. LSTC, 2007.

[12] C. G'Sell, N.A Aly-Helal, and J.J. Jonas. Effect of stress triaxiality on neck propagation during the tensile stretching of solid polymers. *J. of Mat. Sci.*, 18:1731–1742, 1983.

[13] C. G'Sell and J.J. Jonas. Determination of the plastic behaviour of solid polymers at constant true strain rate. *J. of Mat. Sci.*, 14:583–591, 1979.

[14] H. Hansong and T. Ramesh. Numerical simulation of matrix micro cracking in short fibre reinforced polymer composites: initiation and propagation. *Comp. Sci. and Tech.*, 66:2743–2757, 2006.

[15] A. Khan and H. Zhang. Mechanically alloyed nanocrystalline iron and copper mixture: behavior and constitutive modeling over a wide range of strain rates. *Int. J. of Plasticity*, 16(12):1477–1492, 2000.

[16] A. Khan and H. Zhang. Finite deformation of a polymer: experiments and modeling. *Int. J. of Plasticity*, 17(9):1167–1188, 2001.

[17] A.S. Khan and B.F. Farrokh. Thermo-mechanical response of nylon 101 under uniaxial and multi-axial loadings: Part I, Experimental results over wide ranges of strain rates and temperatures. *Int. J. Plasticity*, 22(8):1506–1529, 2006.

[18] A.S. Khan and S. Huang. *Continuum theory of plasticity*. Wiley, New York, 1995.

[19] A.S. Khan and R. Liang. Behaviors of three BCC metal over a wide range of strain rates and temperatures: experiments and modeling. *Int. J. of Plasticity*, 15(10):1089–1109, 1999.

[20] A.S. Khan and R. Liang. Behaviors of three BCC metals during non-proportional multi-axial loadings: experiments and modeling. *Int. J. of Plasticity*, 16(12):1443–1458, 2000.

[21] S. Kolling, A. Haufe, M. Feucht, and P.A. Du Bois. SAMP-1: a semi-analytical model for the simulation of polymers. In *LS-DYNA Conf.* Bamberg, 2005. Paper No. A-II-27.

[22] F. Lauro and J. Oudin. Static and dynamic behaviour of a polypropylene for bumpers. *Int. J. of Crashwortiness*, 8(6):553–558, 2003.

[23] R. Liang and A.S. Khan. A critical review of experimental results and constitutive models for BCC and FCC metals over a wide range of strain rates and temperatures. *Int. J. of Plasticity*, 15(9):963–980, 1999.

[24] Q. Ma, X. Su, X. Lai, J. Lasecki, and R. Frisch. Modeling and simulation of the large deformation behaviour for thermoplastic olefin. *Comp. Mat. Sci.*, 47(3):660–667, 2010.

[25] R.T. Moura, A.H. Clausen, E. Fagerholt, and M. Alves. Impact on HDPE and PVC plates – Experimental and numerical simulations. *Int. J. of Imp. Engng.*, 2010. in press.

[26] A.D. Mulliken and M.C. Boyce. Mechanics of the rate-dependent elastic-plastic deformation of glassy polymers from low to high strain rates. *Int. J. of Solids and Struct.*, 43:1331–1356, 2006.

[27] L. Peroni and M. Avalle. The mechanical behaviour of polyurethane foam in multiaxial loading conditions. In *Proc. IMPLAST 2007*, pages 103–110. Bochum, 2007.

[28] L. Peroni, M. Avalle, and M. Peroni. The mechanical behaviour of aluminium foam structures in different loading conditions. *Int. J. of Impact Eng.*, 35:644–658, 2008.

[29] M. Peroni. *Experimental methods for material characterization at high strain-rate: analytical and numerical improvements*. PhD thesis, Politecnico di Torino, 2008.

[30] M. Peroni, M. Avalle, and L. Peroni. Caratterizzazione dell'influenza della velocità di deformazione sul comportamento meccanico di materiali polimerici. In *Proc. XXXVI AIAS Nat. Conf.*, 2007. Paper No. 106.

[31] M. Peroni and A. Scattina. Modellazione di materiali plastici: creep e sensibilità alla velocità di deformazione. In *Proc. XXXVIII AIAS Nat. Conf.*, 2009. Paper No. 003.

[32] H.J. Qi and M.C. Boyce. Stress-strain behavior of thermoplastic polyurethanes. *Mech. of Mat.*, 37:817–839, 2005.

[33] A.A. Silano, S.K. Bhateja, and K.D. Pae. Effect of hydrostatic pressure on the mechanical behavior of polymers: Polyurethane, poly(oxymethylene), and branched polyethylene. *Int. J. Polymeric Mater*, 3(2):117–131, 1974.

[34] W. Yang and M.X. Chen. Modeling of large plastic deformation in crystalline polymers. *J. of the Mech. and Phys. of Solids*, 49:2719–2736, 2001.

[35] Z.Q. Yu, Q. Ma, X.M. Su, X.M. Lai, and P.C. Tibbenham. Constitutive modeling for large deformation behaviour of thermoplastic olefin. *Materials and Design*, 31(4):1881–1886, 2010.